

# Long-Ranged Electron Interaction between Carboxytetramethylrhodamine and Fluoresceinisoithiocyanate Bound Covalently to DNA, As Evidenced by Fluorescence Quenching

Hiroyuki Kojima,\* Nicolae Spataru,<sup>†</sup> Yoshikazu Kawata, Sin-ichi Yano, and Iuliana Vartires<sup>†</sup>

Osaka National Research Institute, Agency of Industrial Science and Technology, Midorigaoka 1-8-31, Ikeda-shi, Osaka 563, Japan

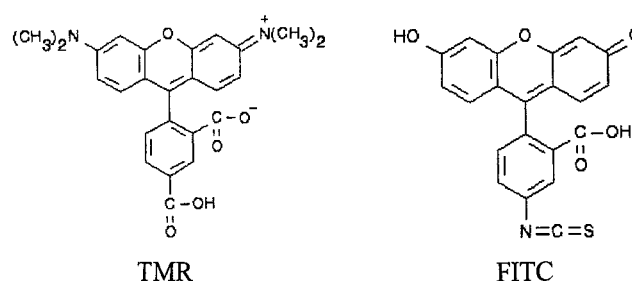
Received: July 2, 1998; In Final Form: October 5, 1998

The fluorescence of 5-carboxytetramethylrhodamine (TMR) and fluoresceinisoithiocyanate (FITC) when bound to double-stranded DNA (dsDNA) residues (24 bp, 138 bp, and 1345 bp) was investigated by steady-state and time-resolved fluorescence measurements. The measurements were carried out using both single-labeled (FITC or TMR) and double-labeled dsDNA (FITC and TMR). A decrease in the fluorescence intensity and lifetime of TMR was observed when a FITC molecule was bound to the opposite end of the nucleic acid structure. Conversely, an increase in the same parameters of FITC was noticed in the double-labeled samples. The addition of pyrrole, an intercalator of DNA, enhanced both effects. These results suggest the existence of an electron interaction between TMR and FITC via long dsDNA coils of over 1000 bp.

Over the past several years, there have been numerous studies of electron-transfer reactions between molecules bound to macromolecular assemblies such as polymers,<sup>1–3</sup> micelles,<sup>4–6</sup> and biomolecules.<sup>7–10</sup> Many of these studies examined possible applications of these reactions to photochemical conversion and storage of solar energy since such reactions may produce long-lived charge separation. Although the process of charge transfer in nucleic acids has been previously postulated,<sup>11,12</sup> only recently has DNA been examined as a medium for electron-transfer reactions.<sup>13,14</sup> Previous studies have shown the feasibility of electron transfer between intercalated reagents,<sup>7,15</sup> between “partially” intercalated transition metal chelates,<sup>13,14</sup> and between intercalated dyes and electron acceptors bound to the outer surface of DNA coils.<sup>16,17</sup> It has been established that in the case of intercalated metal chelates, electron transfer in DNA matrixes can occur efficiently over long distances ( $>40$  Å).<sup>18</sup> Similar results were found using weakly coupled donor–acceptor species intercalated between base pairs in polynucleotides.<sup>7</sup> An effort for elucidating DNA-mediated electron transfer was also dedicated to the electrochemical behavior of DNA-derivatized electrodes.<sup>19</sup> More recently, however, Clegg and co-workers have demonstrated fluorescence resonance energy transfer (FRET) when fluorescein and rhodamine were covalently bound to both 5′ ends of dsDNA ranging from 8 to 20 bp in length.<sup>20</sup> This is a direct electrodynamic interaction between the two dyes, based on the Förster dipole–dipole mechanism, instead of electron transfer. Thus, it was interesting to examine energy transfer between molecules covalently bound to long DNA strands.

Our research investigated by steady-state and time-resolved fluorescence measurements whether electron transfer occurs between donor and acceptor dyes when bound to the opposite ends of long DNA strands. We prepared 24 bp, 138 bp, and 1345 bp dsDNA, labeled with either or both FITC and TMR, using polymerase chain reactions (PCR) with FITC-labeled and/

CHART 1



or TMR-labeled primers. We examined the dependence of DNA chain length and the effect of dye bound at the opposite end, as well as the effect of addition of pyrrole, an intercalator of dsDNA.

## Experimental Section

**Construction of Fluorescently Labeled Double-Stranded DNA Molecules.** The synthesis of fluorescently labeled 138 bp and 1345 bp dsDNA was by PCR using 24-mer primer nucleotides labeled with 5-carboxytetramethylrhodamine (TMR) or fluoresceinisoithiocyanate (FITC) (Chart 1) at the 5′ end (purchased from Synthesgen) or identical primers without label. The primer sequences were 5′-CGCCAGGGTTTCCAGT-CACGAC (named M13FW-TMR, labeled with TMR), 5′-GAG-CGGATAACAATTTACACAGG (M13REV-FITC, labeled with FITC), and 5′-GTCGTGACTGGGAAACCTGGCG (M13FWC-FITC, labeled with FITC). The plasmid pCR II (Invitrogen) inserted with the allophycocyanin genes (DDBJ, EMBL, GeneBank Accession No. D86179) was used as template DNA for PCR. After PCR, the products were purified using a spin column S-400 (Pharmacia, Sweden) to remove unreacted primers. For preparation of 24 bp samples, two primers, M13FW-TMR and M13FWC-FITC, of complementary sequence were carefully annealed. Three different chain length oligo DNA's of 24-mer, 138-mer, and 1345-mer of double-labeled (dl) forms were thus synthesized, together with their

\* Corresponding author. Fax: +81-727-51-9628.

<sup>†</sup> On leave from Institute of Physical Chemistry of the Romanian Academy, 202 Spl. Independentei, 77208 Bucharest, Romania.

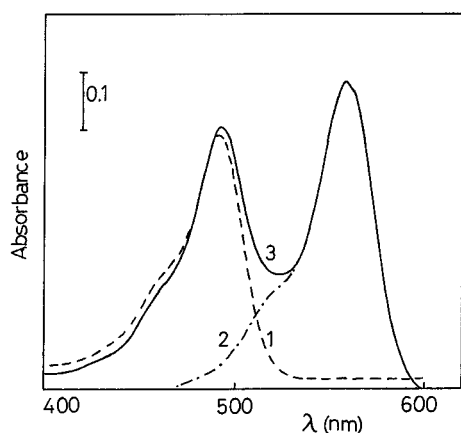


**Figure 1.** Absorption spectra of the FITC-primer (1), TMR-primer (2), and their mixture (3). Concentrations:  $5 \times 10^{-6}$  M.

corresponding single-labeled (sl) form. For single-labeled DNA either TMR or FITC was bound at one 5'-end as fluorescence label, while for the double-labeled DNA both TMR and FITC were bound at the opposite ends of the dsDNA molecules.

**Steady-State Spectroscopy Measurements.** Absorption measurements were taken on a Shimadzu Biospec-1600 spectrophotometer, and results were corrected for the absorption of the corresponding DNA molecules in the absence of dyes. Fluorescence spectra were recorded with a JASCO FP-777 spectrofluorometer. TMR was excited at  $\lambda_{\text{ex}} = 560$  nm, and the fluorescence emission was integrated between  $\lambda_{\text{em}} = 587.5$  and  $687.5$  nm. The wavelength of excitation was  $\lambda_{\text{ex}} = 490$  nm for FITC and its emission was integrated between  $\lambda_{\text{em}} = 525$  and  $625$  nm. All the steady-state spectroscopy measurements were performed in a quartz microcell by using a  $200 \mu\text{L}$  aerated sample.

**Time-Resolved Fluorescence Measurements.** Excited-state lifetimes were determined by the photoelectron counting method using a Horiba NAES-1100 time-resolved spectrofluorometer with a high-pressure hydrogen gas-filled nanosecond lamp. The same volume of sample ( $200 \mu\text{L}$ ) was used for all measurements. The excitation wavelength was tuned to selectively excite either TMR ( $\lambda_{\text{ex}} = 560$  nm) or FITC ( $\lambda_{\text{ex}} = 490$  nm), and fluorescence was separated from scattered light by using appropriate filters. The fluorescence lifetimes were calculated from the fluorescence transient waveform of the sample and the lamp waveform data using the least-squares iterative deconvolution method using computation software provided with the spectrofluorometer. In all cases, the fluorescence lifetimes were analyzed using a two-component exponential function. Reasonable fits were obtained for all the samples, as confirmed both by the plots of residuals differences between experimental emission decays and calculated two-exponential curves and by the reduced  $\chi^2$  statistic ( $\chi^2 < 1.2$ ).

## Results

**Absorption Measurements.** Figure 1 shows the absorption spectra recorded for each of the 24 bp single-stranded nucleotides, either FITC or TMR labeled (curves 1 and 2, respectively), used as primers. The absorption peaks of the two dyes were fairly well separated, even in mixtures of the two primers (curve 3 in Figure 1). This behavior allowed us to selectively excite (in the further fluorescence measurements) either FITC or TMR by using the excitation wavelengths  $\lambda_{\text{ex}} = 490$  and  $560$  nm, respectively. The same spectra, recorded for the single-labeled and double-labeled DNA showed no significant shift

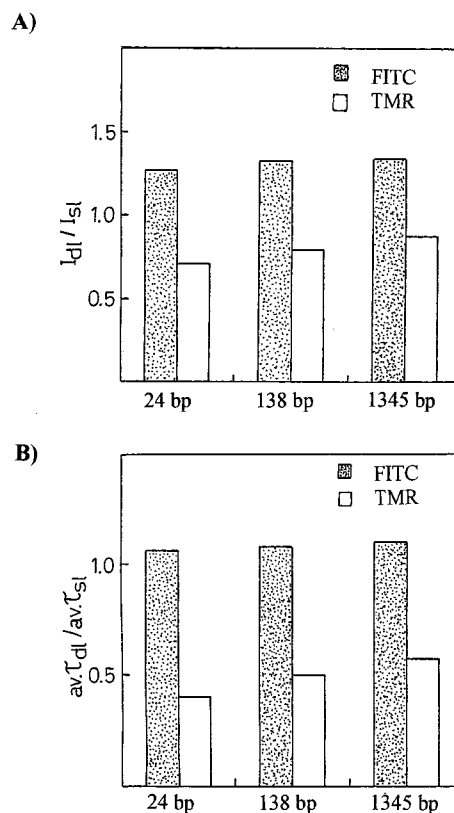


**Figure 2.** Effects of fluorescence of FITC (dotted bar) and TMR (blank bar) on the counterpart dye in the three DNA chain lengths: (a) fluorescence intensity ratio,  $I_{\text{dl}}/I_{\text{sl}}$ , of double-labeled (dl) to single (sl) dsDNA structures; (b) average lifetime ratio,  $\text{av } \tau_{\text{dl}}/\text{av } \tau_{\text{sl}}$  of dl dsDNA to sl dsDNA.

in the absorption maximum position when compared to primers. Therefore, the same wavelengths were used for the excitation of dyes bound to the dsDNA molecules. From the absorption spectra, the molar absorptivities of the two primers were also calculated. Since, due to experimental conditions, the dyes content was not exactly the same in all the samples, these values were used for accurate calculation of the concentrations, starting from absorbance measurements. The absorbance data were corrected for the absorbance of the corresponding dsDNA.

**Steady-State Fluorescence Measurements.** On the basis of the results of the absorption measurements which indicated that the two dyes (FITC and TMR) can be selectively excited, steady-state fluorescence measurements were performed for all the dsDNA molecules, both single- and double-labeled. The emission spectra proved that the fluorescence of FITC and TMR from double-labeled DNA can be separated. Thus, at the excitation wavelength  $\lambda_{\text{ex}} = 490$  nm only the fluorescence of FITC is detected (with the maximum emission around  $\lambda_{\text{em}} = 525$  nm), while exciting at  $\lambda_{\text{ex}} = 560$  nm results in only the detection of the fluorescence of TMR (with a maximum around  $\lambda_{\text{em}} = 580$  nm). For a better interpretation of the results, after integration, the fluorescence intensities were always corrected for the concentration of each dye in the sample, as previously deduced from the absorption measurements. The fluorescence spectra recorded for DNA labeled with either TMR or FITC exhibited a decrease in the integrated fluorescence intensity with an increase in dsDNA residue length.

Steady-state emission measurements of double-labeled dsDNA structures were also performed. Figure 2a shows the ratio between the fluorescence intensity of a dye in a double-labeled sample and their corresponding value for the single-labeled one.

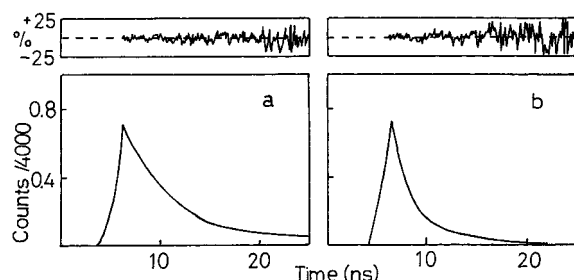


**Figure 3.** Time-resolved single-photon-counting decay profiles, together with weighted residuals, recorded for the single-labeled (FITC) dsDNA molecules: (a) 24 bp; (b) 1345 bp.

Binding a TMR molecule to the opposite end of a FITC-labeled dsDNA resulted in an increase in fluorescence intensity detected for FITC. On the other hand, linking a FITC molecule to the opposite end of a TMR-labeled dsDNA caused a decrease in TMR emission intensity. TMR always exhibited a lower fluorescence intensity in the double-labeled samples, while FITC exhibited higher intensity. This effect was not observed for a mixture of FITC single-labeled dsDNA (24 bp) with TMR single-labeled dsDNA (24 bp) or for a mixture of M13REV-FITC primer with M13FW-TMR primer, of which sequences were not complementary.

**Fluorescence Lifetime Measurements.** Time-resolved fluorescence measurements of TMR conjugated to a 24 bp single-stranded nucleotide (used as a primer) showed fluorescence decay with two distinct lifetimes,  $\tau_{\text{slow}} = 4.07$  ns and  $\tau_{\text{fast}} = 0.31$  ns. This behavior is completely different from that of the free dyes, for which the lifetime data can be fitted well to a one-exponential lifetime.<sup>21</sup> These two observed lifetimes have been previously attributed to at least two species of TMR-DNA that are simultaneously present.<sup>22</sup> A similar two-component fluorescence decay was also found for the 24 bp single-stranded FITC-labeled nucleotide (with  $\tau_{\text{slow}} = 4.23$  ns and  $\tau_{\text{fast}} = 0.37$  ns) and for all the other dsDNA molecules (both single- and double-labeled) used here. The measurements carried out for the single-labeled dsDNA molecules (24 bp, 138 bp, and 1345 bp) clearly showed that the fluorescence decay became faster with increasing DNA chain length. Figure 3 showing the time-correlated single-photon-counting decay profiles recorded for the FITC single-labeled 24 bp and 1345 bp dsDNA (Figure 3a,b, respectively) illustrates this behavior.

Table 1 lists the fluorescence lifetimes of FITC and TMR bound to both single- and double-labeled dsDNA molecules (24 bp, 138 bp, and 1345 bp) together with the relative fluorescence yields (given as decimal fractions in brackets). The bottom line in Table 1 shows the effects of the addition of pyrrole, a DNA intercalator. The ratio of pyrrole to DNA base pairs used was 0.4, on the basis of previous experiments on intercalation of ethidium bromide.<sup>16</sup> Average lifetimes were calculated by summing the products of the emission lifetimes and their corresponding relative fluorescence yield for each dye/dsDNA system to compare dyes. The average lifetimes were correlated with the fluorescence intensity in steady-state measurement with respect to the DNA chain lengths and the effect of the counterpart dye at the opposite end. The addition of pyrrole enhanced the effect of the counterpart dyes. The findings indicate that a decrease in the average lifetimes (for both sl-FITC and sl-TMR dsDNA) induced by increasing the length of the dsDNA is due to a change in the corresponding slow and fast lifetimes relative yields, rather than to a change in  $\tau_{\text{slow}}$  and  $\tau_{\text{fast}}$  values. The same effect was observed for the decrease in the average  $\tau$  of TMR in the presence of the counterpart dye

**TABLE 1: Fluorescence Lifetimes (Nanoseconds) of Dyes Bound to the Double-Stranded DNA Molecules, Single-Labeled (sl) and Double-Labeled (dl)<sup>a</sup>**

DNA	FITC	TMR
24 bp	3.92 [0.75]	3.97 [0.60]
sl	0.26 [0.25]	0.32 [0.40]
	av $\tau$ : 3.00	av $\tau$ : 2.51
138 bp	3.80 [0.25]	4.28 [0.15]
sl	0.25 [0.75]	0.32 [0.85]
	av $\tau$ : 1.14	av $\tau$ : 0.91
1345 bp	3.31 [0.17]	6.05 [0.08]
sl	0.25 [0.83]	0.28 [0.92]
	av $\tau$ : 0.77	av $\tau$ : 0.74
24 bp	3.97 [0.77]	4.17 [0.23]
dl	0.62 [0.23]	0.29 [0.77]
	av $\tau$ : 3.20	av $\tau$ : 1.18
138 bp	3.92 [0.24]	4.57 [0.05]
dl	0.38 [0.76]	0.29 [0.95]
	av $\tau$ : 1.23	av $\tau$ : 0.50
1345 bp	3.28 [0.20]	5.58 [0.03]
dl	0.31 [0.80]	0.27 [0.97]
	av $\tau$ : 0.90	av $\tau$ : 0.43
138 bp, dl	3.65 [0.32]	5.90 [0.02]
+Pyrrole <sup>b</sup>	0.19 [0.68]	0.22 [0.98]
	av $\tau$ : 1.30	av $\tau$ : 0.33

<sup>a</sup> Relative fluorescence yields in the emission decay fit are given as decimal fractions in brackets after the lifetimes. Average emission lifetimes are calculated as the sum of the products of the emission lifetimes and their corresponding relative fluorescence yields. <sup>b</sup> Pyrrole of 0.4 molecule per DNA base pair was added as an intercalator.

(FITC). Figure 2b shows the ratio between the average lifetime of double-labeled and single-labeled dsDNA, which were calculated from Table 1. The results are similar to Figure 2a, although the ratio was shifted to a lower value.

## Discussion

Free TMR in solution forms dimers and higher aggregates that are not fluorescent.<sup>23</sup> Therefore, in the present systems, any direct interactions between the two dyes of the double-labeled samples may not be supposed even for 1345 bp DNA. Fluorescence from the counterpart dye was not detected when one dye is excited in double-labeled dsDNA. This is different from FRET in dsDNA of up to 20 bp.<sup>20</sup>

Quenching of fluorescence in the present system is due to transfer of excited electrons from the dye to DNA and the counterpart dye, because (a) interaction of Foster energy transfer requires sufficient spectrum overlap between the donor and acceptor molecules, but the overlap between FITC and TMR is less than 10%, and (b) it is hard to explain the energy transfer for a long distance in terms of the dipole-dipole interaction because the latter is reduced in proportion to  $R^{-6}$  (the scalar distance between the two molecules). Many dyes displayed striking fluorescence changes upon binding to polynucleotides, and fluorescence quenching on binding to nucleic acids was explained in terms of electron exchange between the excited state of the dye and the ground state of any of the nucleic acid bases.<sup>24–26</sup> The distinct changes of fluorescence by the binding of the counterpart dye in our systems clearly indicate the presence of electron transfer interaction between the two dye molecules covalently bound to both ends of long dsDNA. Our experimental results are summarized as the following:

(1) Fluorescence from FITC or TMR is quenched by long DNA (24 bp to 1345 bp) bound covalently and the quenching is more efficient with increasing DNA chain length.



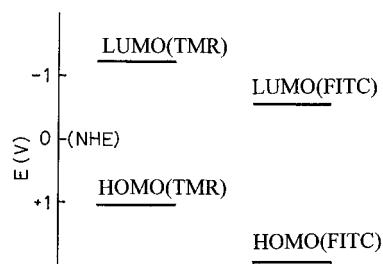


**Figure 4.** Energetic diagram of the lowest unoccupied molecular orbital (LUMO) and the highest occupied molecular orbital (HOMO) of FITC and TMR.

(2) Fluorescence decays biexponentially with the fast component ( $\tau$ : 0.19–0.47 ns) and the slow component ( $\tau$ : 3.28–6.05 ns). Fractions of the fast component increase with increased DNA chain length.

(3) Quenching efficiency is modified by the binding of a counterpart dye molecule at the opposite end of the DNA. Quenching of TMR fluorescence is enhanced by FITC, whereas FITC is slightly reduced by TMR.

(4) The effect of the counterpart dye is enhanced by intercalation of pyrrole into the dsDNA.

Measurements of both steady-state spectroscopy and time-resolved fluorescence gave qualitatively the same results, which is theoretically predicted providing that the radiative lifetime of each component is same. For a two fluorescent component system, the steady-state total fluorescence intensity is proportional to the average fluorescence lifetime by the equation

$$F_{\text{steady-state}} = N_{A+B} \{ \alpha \tau^A + \beta \tau^B \} / \tau_r = N_{A+B} \tau^{\text{av}} / \tau_r$$

where  $N_{A+B}$  is the total number of fluorescent molecules A and B that are excited per unit time,  $\alpha$  and  $\beta$  are the fraction of A and B ( $\alpha + \beta = 1$ ),  $\tau_r$  is the radiative lifetime and  $\tau^{\text{av}}$  is the average lifetime.<sup>22</sup> This relation is approximately true in these systems.

According to Table 1, the dependence of the average lifetime on the DNA chain length is correlated with the change in the fraction of the two decay components. With increasing length, the fast decay component increases. The two components correspond to different forms of electron transfer in dye–DNA conjugate in the excited state, although the mechanisms are unclear.

The effect of the counterpart dye is given by  $I_{\text{dl}}/I_{\text{sl}}$  and  $\text{av } \tau_{\text{dl}}/\text{av } \tau_{\text{sl}}$  in Figure 2a,b. The opposite effect between FITC and TMR may be explained in terms of the electron-accepting (or donating) ability of the counterpart dye molecule. An energy level diagram is schematically shown in Figure 4. Since the redox potential of neither FITC nor TMR has not been reported, the reduction potential of fluorescein (FC) and the oxidation potential of tetraethylrhodamin (TER) are used. Excited electrons go to the lowest unoccupied molecular orbital (LUMO) from the highest occupied molecular orbital (HOMO) and the energy difference is evaluated by the absorption wavelength

(2.22 eV for TMR and 2.53 eV for FITC). We approximated the energy level of the HOMO of TMR from the oxidation potential of TER/TER<sup>+</sup> (+0.77 V vs Ag/Ag<sup>+</sup>(0.01 N) in acetonitrile)<sup>27</sup> and the energy level of the LUMO of FITC from the reduction potential of FC/FC<sup>−</sup> (−0.80 V vs SCE, at pH 7.1).<sup>28,29</sup> In this diagram, only the relative positions of the LUMO level or the HOMO level between FITC and TMR are relevant. The transfer of excited electrons in TMR to DNA is enhanced by the presence of FITC at the opposite end because the LUMO level of FITC is higher than that of TMR. The transfer of excited electrons from FITC to DNA is decreased by the presence of FITC because the LUMO level of FITC is lower than that of TMR. The quenching efficiency is proportional to the driving force of the electron transfer to DNA.

In conclusion, excited electrons of a dye molecule interact with the other dye bound covalently to the opposite end by transfer across over 1000 bp DNA chain.

## References and Notes

- (1) Lehn, J. M. *Angew. Chem., Int. Ed. Engl.* **1990**, 29, 1304.
- (2) Fox, M. A. *Acc. Chem. Res.* **1992**, 25, 569.
- (3) Jones, W. E.; Baxter, S. M.; Strouse, G. F.; Meyer, T. J. *J. Am. Chem. Soc.* **1993**, 115, 7363.
- (4) Davies, K.; Hussam, A. *Langmuir* **1993**, 9, 3270.
- (5) Kuzmin, M. G.; Soboleva, I. V. *J. Photochem. Photobiol. A: Chemistry* **1995**, 87, 43.
- (6) Arkin, M. R.; Stemp, E. D. A.; Turro, C.; Turro, N. J.; Barton, J. K. *J. Am. Chem. Soc.* **1996**, 118, 2267.
- (7) Brun, A. M.; Harriman, A. *J. Am. Chem. Soc.* **1992**, 114, 3656.
- (8) Murphy, C. J.; Arkin, M. R.; Ghatlia, N. D.; Bossmann, S.; Turro, N. J.; Barton, J. K. *Proc. Natl. Acad. Sci. U.S.A.* **1994**, 91, 5315.
- (9) Atherton, S. J.; Beaumont, P. C. *J. Phys. Chem.* **1995**, 99, 12025.
- (10) Netzel, T. L.; Nafisi, K.; Zhao, M.; Lenhard, J. R.; Johnson, I. J. *Phys. Chem.* **1995**, 99, 7936.
- (11) Hoffmann, T. A.; Ladik, J. *Adv. Chem. Phys.* **1964**, 7, 84.
- (12) Dee, D.; Baur, M. E. *J. Chem. Phys.* **1974**, 60, 541.
- (13) Barton, J. K.; Kumar, C. V.; Turro, N. J. *J. Am. Chem. Soc.* **1986**, 108, 6391.
- (14) Purrigan, M. D.; Kumar, C. V.; Turro, N. J.; Barton, J. K. *Science* **1988**, 241, 1645.
- (15) Davis, L. M.; Harvey, J. D.; Baguley, B. C. *Chem.-Biol. Interactions* **1987**, 62, 45.
- (16) Fromherz, P.; Rieger, B. *J. Am. Chem. Soc.* **1986**, 108, 5361.
- (17) Atherton, S. J. *Light in Biology and Medicine*; Douglas, R. H., Moan, J., Dal'Acqua, F., Eds.; Plenum: New York, 1988; Vol. 2, p 77.
- (18) Murphy, C. J.; Arkin, M. R.; Jenkins, Y.; Ghatlia, N. D.; Bossmann, S. H.; Turro, N. J.; Barton, J. K. *Science* **1993**, 262, 1025.
- (19) Kelley, S. O.; Barton, J. K.; Jackson, N.; Hill, M. G. *Bioconjugate Chem.* **1977**, 8, 31.
- (20) Clegg, R. M.; Murchie, A. I. H.; Zechel, A.; Lilley, D. M. J. *Proc. Natl. Acad. Sci. U.S.A.* **1993**, 90, 2994.
- (21) Vogel, M.; Rettig, W.; Sens, R.; Drexhage, K. H. *Chem. Phys. Lett.* **1988**, 147, 452.
- (22) Vamosi, G.; Gohlke, C.; Clegg, R. M. *Biophys. J.* **1996**, 71, 972.
- (23) Kemnitz, K.; Tamai, N.; Yamazaki, Y.; Nakashima, N.; Yoshihara, K. *J. Phys. Chem.* **1986**, 90, 5094.
- (24) Kittler, L.; Löber, G. *Photochemical and Photobiological Reviews*; Smith, K. C., Ed.; Plenum Press: New York, 1977, Vol. 2, p 39.
- (25) Löber, G.; Kittler, L. *Photochem. Photobiol.* **1977**, 25, 215.
- (26) Kittler, L.; Löber, G.; Gollmick, F. A.; Berg, H. *J. Electroanal. Chem.* **1980**, 116, 503.
- (27) Takizawa, T.; Watanabe, T.; Honda, K. *J. Phys. Chem.* **1978**, 82, 1391.
- (28) Delahay, P. *Bull. Soc. Chim. Fr.* **1948**, 348.
- (29) Rehm, D.; Weller, A. *Ber. Bunsen-Ges. Phys. Chem.* **1969**, 73, 834.